Soft Matter

Dynamic behavior of chemically tunable mechano-responsive hydrogels

Journal:	*Soft Matter*
Manuscript ID	SM-ART-08-2021-001188.R1
Article Type:	Paper
Date Submitted by the Author:	02-Nov-2021
Complete List of Authors:	Biswas, Santidan; University of Pittsburgh, Chemical Engineering Yashin, Victor; University of Pittsburgh, Balazs, Anna; University of Pittsburgh, Chemical Engineering

Dynamic behavior of chemically tunable mechano-responsive hydrogels

Santidan Biswas, Victor V. Yashin, Anna C. Balazs*

Chemical Engineering Department, University of Pittsburgh, Pittsburgh, PA 15261,

United States

* balazs@pitt.edu

Abstract

Using theory and simulation, we model the mechanical behavior of gels that encompass loops and dangling chain ends. If the loops remain folded and dangling ends are chemically inert, then these topological features just serve as defects. If, however, the loops unfold to expose the hidden ("cryptic") binding sites and the ends of the dangling chains are reactive, these moieties can form bonds that improve the gel's mechanical properties. For gels with a lower critical solubility temperature (LCST), we systematically switch on the possible unfolding and binding events. To quantify the resulting effects, we derive equations for the gel's equilibrium and dynamic elastic moduli. We also use a finite element approach to simulate the gel's response to deformation and validate the analytic calculations. Herein, we show that the equilibrium moduli are highly sensitive to the presence of unfolding and binding transitions. The dynamical moduli are sensitive not only to these structural changes, but also to the frequency of deformation. For example, when reactive ends bind to exposed cryptic sites at $T = 29°\mathrm{C}$ and relatively high frequency, the storage shear modulus is 119% greater than the corresponding equilibrium value, while the storage Young's modulus is 109% greater than at equilibrium. These findings provide guidelines for tuning the chemical reactivity of loops and dangling ends and the frequency of deformation to tailor the mechano-responsive behavior of polymer networks.

I. Introduction

Polymer gels typically contain topological "defects",[1]including both loops and dangling chains. If the loops are permanently closed and the dangling chains are chemically inert, then these features do not contribute to variations in the elasticity of network as the material undergoes deformations, and hence, are effectively wasted with respect to tuning the dynamic properties of a gel.[2] On the other hand, if the loops unravel to expose buried binding sites (i.e., "cryptic" sites[3,4]) and the dangling chains include reactive end groups (Fig. 1), then the system can form new bonds, which will affect the material's global response to deformation. Here, we derive expressions to analyze how the equilibrium shear, bulk and Young's moduli, which characterize the stiffness of the material, depend on the chemical reactivity of the loops and dangling chains. Consequently, we can determine how to exploit these defects to tailor the materials' equilibrium behavior. To understand how these materials respond to time-dependent deformations, we also derive expressions for the dynamic moduli when this material is subjected to oscillatory deformation. To verify the results obtained from the analytic calculations, we carry out simulations on a single element of the gel using the gel lattice spring model (gLSM)[5–7], which utilizes a finite element approach to characterize the materials properties. Taken together, these studies provide guidelines for tuning the time-dependent deformations and the reactivity of topological defects to achieve the desired mechanical properties for a wide breadth of applications.

We specifically focus on the gel systems depicted in Fig. 2, where all the gels encompass the same structural elements, i.e., loops and dangling chains in polymer strands that lie between two consecutive, permanent crosslinks. Using our analytical model, we specify that the loops can

unfold and refold with certain probabilities, which depend on the state of deformation. We also specify the strain-dependent probabilities of the binding and unbinding between the exposed cryptic sites and the reactive ends groups. As illustrated in Fig. 2, we systematically switch on and off various structural transformations in the gel to pinpoint how different folding and binding events contribute to the mechanical responses of the material to static and dynamic deformations.

The gel in our system is taken to be poly(N-isopropylacrylamide) (pNIPAAm), which exhibits a lower critical solution temperature (LCST)[8]. Hence, the gel shrinks above the volume phase transition temperature (T_c), which is approximately 33°C for pNIPAAm, and swells in volume as the temperature is lowered below T_c. Notably, we observe a crossover temperature, T_s, beyond which the mechanical stiffness of the gels with no binding and unfolding and the gels with all possible binding and unfolding events undergo an exchange in mechanical behavior. (Note the crossover temperature T_s is different for the shear modulus and the bulk modulus.) Interesting, for $T < T_s$, the permanently folded gel has a higher moduli than the gel undergoing both folding and binding.

We also observe intriguing behavior in analyzing the frequency dependent response of the gel systems (in the limit of small deformation). In particular, we find that the isothermal frequency scans for the shear moduli show no dependence in the mechanical property for the systems, where the dangling chains do not undergo binding. For the dynamic Young's modulus, the sample undergoing folding and/or binding shows a dependence on frequency only at high frequency values, as the frequency dependent response depends on the kinetic rate constants of folding and binding.

We emphasize that although the gel samples all have the same elements or units i.e. the loops (cryptic sites) and dangling linkers, the dynamic behavior of the gel can be finely tuned by

tailoring the chemical reactivities[9] of these units and hence, modify the mechanical response of the system. The permissibility of some transitions to happen and inhibiting some transitions lead to different mechanical response of such gel system (see Fig.2). This can help in creating synthetic materials having the basic elements but based on the need of the material property, the reactivity of these units can be turned on or off like a switch.

Through these studies, we devise an approach for creating materials with hidden length or materials that can exhibit self-stiffening or self-reinforcing behavior. Namely, by tuning the chemical reactivity of the units making up the gel sample, a variety of mechano-responsive behaviors could be achieved. Our theory can provide guidelines in designing materials with desired mechanical properties.

II. Methodology

Before detailing the specifics of our calculations, we provide an outline of our approach to facilitate the ensuing discussion. To obtain the analytical expressions for the equilibrium shear and bulk moduli, we carry out linearization of the stress tensor around the steady state (equilibrium solution of the gel system i.e., when the total stress on the system is zero) at a given temperature. From linear elasticity[10], the linearization of the stress tensor yields the Lamé constants; these Lamé constants are related to the shear and bulk modulus. The equilibrium shear modulus is obtained from the contributions to the stress tensor that are linear in strain. The resulting expression for the shear modulus only depends on the equilibrium swelling properties of the gel system at the given temperature. Thus, knowing the equilibrium properties of the swollen gel, equilibrium kinetic values, such as probability of unfolding and binding, can directly yield the value of the shear modulus. The bulk modulus describes the response of the system when it is uniformly deformed in all directions, and hence the system changes volume. For the calculation of the bulk modulus,

we consider the spatially isotropic contribution to the stress tensor due to variation in volume. The volumetric stress shows dependence on the linearized variations of the kinetics of folding and binding, and the value of the equilibrium bulk modulus is calculated accordingly. The Young's modulus is related to the shear and bulk moduli, and is thus obtained indirectly once the values of the shear and bulk moduli are obtained numerically.

As a mode of verification, we carry out single element gLSM simulations to obtain the equilibrium moduli. Thus, for the equilibrium moduli, in the gLSM simulation, we carry out strain-controlled deformations. First, we calculate the equilibrium shear modulus, which describes the system's response to a deformation applied parallel to one surface (e.g., the top of a rectangular object), while the opposite surface (the bottom) is held fixed. This deformation leads to a change in shape, while the volume remains constant. In a gLSM simulation, instead of computing bulk moduli, which would require isotropic compression of the gel sample from all sides, we directly carry out simulations to characterize the stiffness of the system (Young's modulus) by applying a tensile deformation. The sample is pulled along a surface by a small amount (e.g., the top face), while the bottom face is held fixed. The faces on the sides of the rectangular sample move in response to the deformation. By calculating the force normal to the top face and dividing by the applied strain, we can calculate the equilibrium Young's modulus. Note the volume is not preserved in tensile deformation.

The dynamic moduli depend on both temperature and the frequency. The linearized stress-strain is calculated by applying a Fourier transform, and in this scenario, the Lamé constants become the convolution kernels. In particular, equating these Fourier transformed expressions, we calculate the dynamic shear modulus and the dynamic bulk modulus. From the latter values, we obtain the dynamic Young's modulus, which characterizes the system's response to tensile

deformation. Using these expressions for the different moduli, we calculate the storage modulus. We also carry out single element gLSM simulations to calculate the dynamic shear modulus where the deformation applied was similar to the equilibrium scenario i.e. deforming the top face and keeping the bottom face fixed. To obtain the dynamic modulus, the deformation applied is a cyclic sinusoidal deformation. The amplitude of deformation was kept small, ~1% strain, to ensure that the strain applied is in the linear elasticity regime. The dynamic response of the gel depends on the formation and breaking of temporary crosslinks, which depend on the past history of deformation through the relative strain tensor. In the gLSM simulations, accounting for the temporary crosslink contribution thus requires storing large data sets and becomes computationally intensive. Also, the shear deformation is a volume preserving deformation. As a demonstration, we thus only carry out simulations to calculate the shear modulus. We also derive the analytical value of stress for the case of simple shear and tensile deformation in the Supplementary Information (the SI, Section S5).

A. Theoretical model

We utilize our recently developed model for permanently cross-linked, swollen polymer gels that encompass loops and dangling chains that act together to re-inforce the network in response to deformation[11] . In the previous studies, we focused solely on the case where the ends of the dangling chains are chemically reactive and bind reversibly to the exposed cryptic sites, thus forming additional temporary crosslinks. In Fig. 1, this polymer network is drawn in green and the permanent cross-links are shown in grey. The ends of the dangling chains are capped by reactive sites (in yellow) and can bind to the exposed red sites. The sites that are chemically inert are shown in black. We demonstrated that a decrease in temperature or an applied force can drive the loops

in this LCST gel to unfold and expose the red sites. We referred to the red sites as "cryptic" sites because they are hidden unless the gel is deformed. When the exposed cryptic sites bind to the reactive yellow ends, the equilibrated structure displays "struts" that reinforce the network, as indicated by a significant decrease in the volume of the gel and shifts in volume phase transition temperature. Notably, the decrease in volume can range from 44% to 80% of the initial volume (see below). Once the temperature is increased or the deformation is removed, the reversible bonds with the dangling chains are broken, the loops refold and the gel returns to its original state. In this way, the system can repeat this self-reinforcing behavior in response to later perturbations.

In the present study, we go beyond this one case and consider how the reactivity of the different potential binding sites affects the overall mechanical properties. Within all the cases examined here, the loops are assumed to be closed in the as-fabricated gel. Every subchain in the network contains $n+l$ Kuhn segments; for subchains containing loops, the l segments lie within the loop. The dangling chains contain m Kuhn segments. We assume that the time scale for the breaking and reforming of a bond between the reactive groups (red-red or red-yellow) is longer than the time scale associated with the conformational changes of the chain. In this case, the binding and unbinding, as well as the folding and unfolding, can be described by the equations for the chemical kinetics in the network.

Given the presence of these different reactive sites, we anticipate that the dynamic behavior of the gel can be finely tuned by tailoring the chemical reactivities[9,12,13] and hence, the possible binding interactions within the system. To test this hypothesis, we now consider four different scenarios that can be attained by chemically modifying the reactive species. The four scenarios are:

System I: The ends of the dangling chains are chemically non-reactive, so they cannot participate in binding. The loops are permanently in the unfolded (open) conformation and the exposed sites do not react with the inert dangling ends.

System II: The ends of the dangling chains are chemically inert but the cryptic sites in the loops are reactive, so the loops can undergo the reversible folding-unfolding transformations.

System III: The cryptic sites form permanent bonds with each other and maintain the loop in the folded state, so that binding of the dangling chains cannot occur.

System IV: The ends of the dangling chains are chemically reactive and can bind reversibly to the exposed cryptic sites, thus forming additional temporary crosslinks. The loops can also undergo reversible folding and unfolding. The equilibrium behavior of this system was described in ref. [11].

At the outset, we define the relevant parameters and state the simplifying assumptions in the model. (Since the model builds on our previous work,[11] we provide further details in the SI.) Here, c_l and c_d denote the respective concentration of subchains encompassing the loops and dangling chains. Given p_U is the fraction of subchains with unfolded loops, the total concentration of the exposed cryptic sites is $n_c = 2 p_U c_l$. The parameter π_B is the fraction of exposed cryptic sites that are bound to the dangling chains and hence, the concentration of the latter sites is $n_c^{(b)} = \pi_B n_c$. We assume that there are two dangling chains per subchain and hence, the total concentration of the reactive end-units is $n_d = 2c_d$. The concentration of end-units (and hence, dangling chains) bound to the cryptic sites is $c^* = p_B n_d$, where p_B is the fraction of bound dangling chains. Since $n_c^{(b)} = c^*$, then $\pi_B p_U c_l = p_B c_d$. Lastly, the amount of the subchains encompassing loops is equal to the amount encompassing dangling chains. Notably, the network

does not contain other types of subchains. For these cases, $c_l = c_d = 2^{-1}\phi_0^{-1}\phi c_0$, where, c_0 and ϕ_0 are the respective concentrations of polymer strands and the volume fraction of polymer in the undeformed network. The volume fraction of polymer in the deformed state of the system is ϕ. Notably, in the theory of rubber elasticity, the cross-link density, c_0, (by definition) characterizes the undeformed sample. The value $c^* = \phi_0^{-1}\phi c_0 p_B$ is hence interpreted as the density of temporary cross-links.

The fraction of unfolded loops, p_U, as a function of time t is described by the following rate equation:

$$dp_U/dt = k_r (1 - p_U) - k_f (1 - \pi_B)^2 p_U \qquad (1)$$

where, $k_r(R) = k_r^{(0)} \exp[\gamma_R F_n(R)/k_B T]$ and $k_f(R) = P_c(R) k_f^{(0)}$ are the respective rate constants for the rupture and formation of the labile bond between two cryptic sites. The values of k_r and k_f depend on the distance (R) between the ends of the subchain that form the loop, as discussed in detail below. $k_r^{(0)}$ is the rate of rupture at zero force, and $F_n(R)$ is the force applied to the ends of a chain of n segments. Additionally, γ_R characterizes the sensitivity of the bond to the applied force; k_B and T are the respective Boltzmann's constant and temperature. The probability of contact of the loop ends is given by $P_c(R)$ and $k_f^{(0)}$ is the rate of rupture at zero force. Further details are provided in Sec. S1 of the SI.

Equation (1) is a modification of the equation in our model for polymer chains with loops developed previously.[14] For simplicity, we ignore the formation of labile bonds between two exposed cryptic sites that belong to different subchains. When the loops unfold, the end-groups of

the dangling chains can bind to the exposed cryptic sites (Fig. 1). The reaction rate constants for the complex formation, $K_{compl}(\phi) = K_0 \exp[-(a_0/b)^{4/3}(n+m+l)^{-1/3}\phi^{-2/3}]$, and the unbinding of the loops, $K_{uB}(R) = k_{uB}^{(0)}\exp[\gamma_{uB} F_m(R)/k_B T]$, depend on the network structure and state of deformation.[11] K_0 is the rate constant of complex formation, a_0 is the size of a monomer, b is the Kuhn length, $k_{uB}^{(0)}$ and γ_{uB} are the respective reaction rate constant at zero force and the force sensitivity parameter, and $F_m(R)$ is the force applied to the ends of a chain of m segments. The rate equation for the fraction of bound dangling chains, p_B is written as

$$dp_B/dt = \phi_0^{-1}\phi c_0 K_{compl} p_U (1-\pi_B)(1-p_B) - K_{uB} p_B \qquad (2)$$

At a constant degree of swelling, ϕ is a constant; the values p_U and p_B are obtained by solving the combination of eqs. (1) and (2). Note that the fraction of cryptic sites bound to the dangling chains, π_B, is not an independent variable and is obtained from $p_B = \pi_B p_U$. The detailed expressions for the rate constants are provided in Sec. S1 of the SI.

B. Modeling the dynamic response of the gel to deformation

To describe the dynamic behavior of the material under deformation, we characterize the properties of the system at two moments of time, τ and t. In particular, we determine $\bar{\lambda}(t,\tau)$ by averaging the relative principal strains, namely, $\bar{\lambda}(t,\tau) = 3^{-1/2}\sqrt{\sum_{i=1}^{3}\lambda_i^2(t)\lambda_i^{-2}(\tau)}$, where $\lambda_i(\tau)$ and $\lambda_i(t)$, $i = 1,2,3$, are the principal strains calculated at the moments of time τ and t, respectively. Additionally, we calculate the function $\xi(t,\tau)$, which determines the number of cross-links that were created before the time τ and still exist at time $t \geq \tau$. The time derivative $\partial\xi(t,\tau)/\partial\tau$ determines the number of cross-links that exist at time t and were created during the

period of time from τ to $\tau + d\tau$. To specify the functions $\xi(t,0)$ and $\partial\xi(t,\tau)/\partial\tau$, we write the formal solution of eq. (2) for the fraction of bound dangling chains p_B:

$$p_B(t) = p_B(0)\exp[-\int_0^t K_{uB}(\tau,0)d\tau] + \int_0^t \exp[-\int_\tau^t K_{uB}(\tau',\tau)\,d\tau']K_B(\tau)d\tau \tag{3}$$

In the above equation, the rate of binding $K_B(t)$ is defined as

$$K_B = c_0\,\phi_0^{-1}\phi\,K_{compl}(\phi)(1-p_B)(p_U - p_B) \tag{4}$$

and depends on time t through the time-dependent fractions of unfolded loops, p_U, and bound dangling chains, p_B, and the time-dependent volume fraction of polymer, ϕ. Correspondingly, the functions $\xi(t,0)$ and $\partial\xi(t,\tau)/\partial\tau$ are calculated as

$$\xi(t,0) = p_B(0)\exp[-\int_0^t K_{uB}(\tau,0)d\tau] \tag{5}$$

$$\frac{\partial\xi}{\partial\tau}(t,\tau) = \exp[-\int_\tau^t K_{uB}(\tau',\tau)\,d\tau']K_B(\tau) \tag{6}$$

The rate constant of unbinding $K_{uB}(t,\tau)$ in eqs. (5) and (6) is calculated according to eq. (S1.6) in the SI, and depends on both the time t and the time of bond creation $\tau \le t$. The latter dependence arises because a newly formed cross-link experiences no force at the moment of creation τ, and the force acting on it at the time t depends on the relative chain extension $\lambda(t,\tau)$.

The constitutive equation that provides the stress-strain relationships in the material is formulated[11,14,15] from the free energy density (see Sec. S2 of the SI for details) to obtain the following equation for the stress tensor $\hat{\boldsymbol{\sigma}}$:

$$\hat{\boldsymbol{\sigma}} = \hat{\boldsymbol{\sigma}}_{\mathrm{el}} - \pi_{\mathrm{FH}}(\phi,T)\hat{\mathbf{I}} + \hat{\boldsymbol{\sigma}}^*_{\mathrm{el}}(t) \tag{7}$$

where $\hat{\mathbf{I}}$ is the unit tensor. It is convenient to introduce the function $\zeta(x)$ defined as $\zeta(x) = (3x)^{-1}\mathcal{L}^{-1}(x)$ and $\zeta_0(n) = \zeta(n^{-1/2})$, where $\mathcal{L}(x)$ is the Langevin function. We express $\hat{\boldsymbol{\sigma}}_{\text{el}}$, the elastic stress due to the freely jointed chains (FJC), in terms of these variables:

$$\begin{aligned}\hat{\boldsymbol{\sigma}}_{el} = \frac{c_0 v_0}{2}\Bigg[(1-p_U)\,\zeta\left(\frac{\bar{\lambda}}{\sqrt{n}}\right) + p_U\,\zeta\left(\frac{\bar{\lambda}\sqrt{n}}{n+l}\right) + \zeta\left(\frac{\bar{\lambda}}{\sqrt{n+l}}\right)\Bigg]\frac{\phi}{\phi_0}\hat{\mathbf{B}} \\ - c_0 v_0[\zeta_0(n) + \zeta_0(n+l)]\frac{\phi}{4\phi_0}\hat{\mathbf{I}}\end{aligned} \tag{8}$$

In eq. (7), $\pi_{\text{FH}}(\phi, T)$ is the osmotic pressure of the polymer in the system according to the Flory-Huggins model

$$\pi_{\text{FH}}(\phi, T) = -[\phi + \log(1-\phi) + \chi(\phi, T)\phi^2] \tag{9}$$

The interaction parameter $\chi(\phi, T)$ is related to the Flory-Huggins interaction parameter $\chi_{FH}(\phi, T)$ as $\chi(\phi, T) = \chi_{FH}(\phi, T) + (1-\phi)\partial_\phi \chi_{FH}(\phi, T)$. The last term in eq. (7) is the elastic stress due to the temporary cross-links:

$$\begin{aligned}\hat{\boldsymbol{\sigma}}^*_{\text{el}}(t) = c_0 v_0 \xi(t,0)\frac{\phi}{\phi_0}\left[\zeta\left(\frac{\bar{\lambda}(t,0)}{\sqrt{m}}\right)\hat{\mathbf{b}}(t,0) - \frac{\zeta_0(m)}{2}\hat{\mathbf{I}}\right] + \\ + c_0 v_0 \frac{\phi}{\phi_0}\int_0^t \frac{\partial \xi}{\partial \tau}(t,\tau)\left[\zeta\left(\frac{\bar{\lambda}(t,\tau)}{\sqrt{m}}\right)\hat{\mathbf{b}}(t,\tau) - \frac{\zeta_0(m)}{2}\hat{\mathbf{I}}\right]d\tau\end{aligned} \tag{10}$$

The equilibrium swelling of a gel that contains both cryptic bonds and dangling chains with reactive ends is determined by solving eqs. (1), (2), and (7) in the steady-state limit, i.e., by solving the system of equations $dp_U / dt = 0$, $dp_B / dt = 0$, and $\hat{\boldsymbol{\sigma}} = \mathbf{0}$. To determine the equilibrium value of $\hat{\boldsymbol{\sigma}}^*_{\text{el}}$, we note that $\xi(t,0) \to 0$ at $t \to \infty$, and that $\hat{\mathbf{b}}(t,\tau) = \hat{\mathbf{I}}$ and $\bar{\lambda}(t,\tau) = 1$ at equilibrium.

According to eqs. (3), (5), and (6), the probability of binding can be calculated as $p_B(t) = \xi(t,0) + \int_0^t \frac{\partial \xi}{\partial \tau}(t,\tau) d\tau$. Then, the following equilibrium limit of eq. (10) is given as:

$$\hat{\boldsymbol{\sigma}}^*_{\mathrm{el}} = p_B c_0 v_0 \phi (2\phi_0)^{-1} \zeta_0(m) \hat{\mathbf{I}} \tag{11}$$

Finally, we note that the equilibrium value of the rate constant of unbinding K_{uB}, eq. (S1.6), should be calculated at the chain extension $\bar{\lambda} = 1$, because K_{uB} depends on the relative strain.

C. Dynamic elastic moduli of the gel

In addition to parameters characterizing the gel's structural composition, we determine the gel's mechanical properties, which depend on temperature and frequency of the deformation. Similar to an isotropic solid, the gel systems can be characterized by two elastic constants: the shear and the bulk moduli. The shear modulus describes the system's response to shearing and the bulk modulus describes the material's response to uniform deformation along all directions. To characterize these mechanical properties, we perform a linearization of the constitutive equations around the steady state of the gel, i.e. $\hat{\boldsymbol{\sigma}} = 0$. In the absence of relaxation, linearization of the stress tensor results in

$$\delta\hat{\boldsymbol{\sigma}}(t) = \lambda \,\mathrm{tr}[\hat{\boldsymbol{\varepsilon}}(t)]\hat{\mathbf{I}} + 2\mu\,\hat{\boldsymbol{\varepsilon}}(t) \tag{12}$$

where λ and μ are the first and second Lamé parameters, respectively, and $\hat{\boldsymbol{\varepsilon}}$ is the infinitesimal strain tensor. (Note that in eqs. (12)-(15), we use the symbol λ for the first Lamé parameter according to tradition. For the rest of the paper, the symbol λ is reserved for the degree of swelling.)

If relaxation takes place, the Lamé parameters become the convolution kernels, and the stress-strain equation is conveniently formulated via the Fourier transform:

$$\delta\hat{\boldsymbol{\sigma}}_\omega = \lambda_\omega \,\mathrm{tr}(\hat{\boldsymbol{\varepsilon}}_\omega)\hat{\mathbf{I}} + 2\mu_\omega\,\hat{\boldsymbol{\varepsilon}}_\omega \tag{13}$$

The Fourier transform is defined here as $f_\omega = \int_{-\infty}^{+\infty} f(t)\exp(-i\omega t)dt$. The (complex) dynamic shear G_ω and bulk K_ω moduli are related to the Lamé parameters as[10]

$$G_\omega = \mu_\omega \tag{14}$$

$$K_\omega = \lambda_\omega + \frac{2}{3}\mu_\omega \tag{15}$$

The dynamic Young's modulus of the gel E_ω is calculated through the shear and bulk moduli as[10]

$$E_\omega = \frac{9K_\omega G_\omega}{3K_\omega + G_\omega} \tag{16}$$

The frequency-dependent storage and loss moduli are given by the respective real and imaginary parts of eqs. (14)-(16). Recall that the storage modulus characterizes the energy stored in the material and the loss modulus characterizes the energy dissipated by the system (e.g., as heat). Finally, the equilibrium values of the elastic moduli are obtained by taking the limit $\omega \to 0$ in eqs. (14)-(16). Section S4 of the SI provides detailed derivations of the dynamic moduli of the gel.

The elastic moduli of a swollen gel depend on the frequency of deformation, ω, due to the volumetric and chemical relaxation processes in the system. In the case of simple shear deformation, only chemical relaxation takes place in the gel because volume does not change under shear. The storage and loss shear moduli, G' and G'', respectively, are given by the following equations (see Section S4 in the SI):

$$G'(\omega) = G_0 + \Delta G \frac{(\omega / K_{uB}^{(st)})^2}{1 + (\omega / K_{uB}^{(st)})^2} \tag{17}$$

$$G''(\omega) = \Delta G \frac{\omega / K_{uB}^{(st)}}{1 + (\omega / K_{uB}^{(st)})^2} \tag{18}$$

In eq. (17), G_0 is the equilibrium shear modulus calculated as

$$G_0 = \frac{c_0}{2\lambda_{st}}\left[(1-p_U^{(st)})\,\zeta\left(\frac{\lambda_{st}}{\sqrt{n}}\right)+p_U^{(st)}\,\zeta\left(\frac{\lambda_{st}\sqrt{n}}{n+l}\right)+\zeta\left(\frac{\lambda_{st}}{\sqrt{n+l}}\right)\right] \tag{19}$$

The subscripts and superscripts "st" denote a steady state value at a given temperature T. The equilibrium shear modulus is proportional to the crosslink density c_0, and depends on the degree of swelling λ_{st} and fraction of unfolded loops $p_U^{(st)}$ at the steady state. The value ΔG in eqs. (17) and (18) characterizes contribution of the relaxation processes to the dynamic shear modulus

$$\Delta G = c_0\zeta_0(m)\frac{\phi_{st}}{\phi_0}p_B^{(st)} \tag{20}$$

where $p_B^{(st)}$ is the fraction of bound dangling chains in the steady state. Equation (20) shows that only dangling chains bound to the exposed cryptic sites contribute to the dynamic shear modulus. Namely, shear affects the temporary crosslinks. Finally, as seen from eqs. (17) and (18), the characteristic relaxation time associated with the bound dangling chains is $1/K_{uB}^{(st)}$, where $K_{uB}^{(st)}$ is the steady state value of the reaction constant for unbinding.

To calculate the bulk modulus, we consider the spatially isotropic contributions to the stress tensor due to variations of volume:

$$\begin{aligned}\delta\hat{\boldsymbol{\sigma}}^{(v)}(t) = &\left[-\phi_{st}\left(\frac{\partial\sigma_{vol}}{\partial\phi}\right)_{st}+\frac{\lambda_{st}}{3}\left(\frac{\partial\sigma_{vol}}{\partial\bar{\lambda}}\right)_{st}\right]\mathrm{tr}[\hat{\boldsymbol{\varepsilon}}(t)]\hat{\mathbf{I}}\\ &+\left[\left(\frac{\partial\sigma_{vol}}{\partial p_U}\right)_{st}\delta p_U(t)+\left(\frac{\partial\sigma_{vol}}{\partial p_B}\right)_{st}\delta p_B(t)\right]\hat{\mathbf{I}}\end{aligned} \tag{21}$$

where,

$$\begin{aligned}\sigma_{vol} = &\frac{c_0\lambda_{st}^2}{2}\frac{\phi}{\phi_0}\left[(1-p_U)\,\zeta\left(\frac{\bar{\lambda}}{\sqrt{n}}\right)+p_U\,\zeta\left(\frac{\bar{\lambda}\sqrt{n}}{n+l}\right)+\zeta\left(\frac{\bar{\lambda}}{\sqrt{n+l}}\right)\right]\\ &+c_0\,\zeta_0(m)\,p_B\frac{\phi}{2\phi_0}-\left(\pi_{FH}(\phi)+c_0[\zeta_0(n)+\zeta_0(n+l)]\frac{\phi}{4\phi_0}\right)\end{aligned} \tag{22}$$

Equation (21) indicates that the volumetric stress is also affected by the unfolding and binding processes occurring in the gel, as expressed through the terms proportional to $\delta p_U(t)$ and $\delta p_B(t)$, respectively. Linearization of the non-linear chemical kinetics equations for p_U and p_B results in the following linear equations for δp_U and δp_B which, in turn, are linear functionals of $\mathrm{tr}\,\hat{\boldsymbol{\varepsilon}}(t)$.

$$\frac{d}{dt}\begin{pmatrix}\delta p_U\\ \delta p_B\end{pmatrix}+\begin{pmatrix}\Gamma_{UU} & \Gamma_{UB}\\ \Gamma_{BU} & \Gamma_{BB}\end{pmatrix}\begin{pmatrix}\delta p_U\\ \delta p_B\end{pmatrix}=\begin{pmatrix}\delta K_U\\ \delta K_B\end{pmatrix}\mathrm{tr}\,\hat{\boldsymbol{\varepsilon}}(t)$$

A detailed discussion of the above expressions is given in Section S4 of the SI.

For the dynamic moduli, the equations for δp_U and δp_B are solved in terms of the Fourier transforms:

$$\begin{pmatrix}\delta p_{U\omega}\\ \delta p_{B\omega}\end{pmatrix}=(i\omega\hat{\mathbf{I}}+\hat{\boldsymbol{\Gamma}})^{-1}\begin{pmatrix}\delta K_U\\ \delta K_B\end{pmatrix}\mathrm{tr}\,\hat{\boldsymbol{\varepsilon}}_{\omega}$$

Finally, the complex dynamic bulk modulus K_ω is expressed in the following form:

$$\begin{aligned}K_\omega=&\left(\phi^2\frac{\partial}{\partial\phi}\left(\frac{\pi_{FH}}{\phi}\right)+\frac{\bar{\lambda}}{3}\frac{\partial\sigma_{vol}}{\partial\bar{\lambda}}\right)_{st}\\&+\begin{pmatrix}\left(\frac{\partial\sigma_{vol}}{\partial p_U}\right)_{st} & \left(\frac{\partial\sigma_{vol}}{\partial p_B}\right)_{st}\end{pmatrix}(i\omega\hat{\mathbf{I}}+\hat{\boldsymbol{\Gamma}})^{-1}\begin{pmatrix}\delta K_U\\ \delta K_B\end{pmatrix}\\&+\frac{2}{3}G_\omega\end{aligned}\qquad(23)$$

The above equations show that the dynamic bulk modulus K_ω has three characteristic frequencies:

$$\omega_0^{(1,2)}=\frac{\Gamma_{UU}+\Gamma_{BB}}{2}\pm\frac{1}{2}\left((\Gamma_{UU}-\Gamma_{BB})^2+4\Gamma_{UB}\Gamma_{BU}\right)^{1/2},\ \omega_0^{(3)}=K_{uB}^{(st)}\ .$$

Thus, the bulk modulus not only depends on the volume fraction ϕ, but also on the steady state value of the reaction constant for unbinding and unfolding.

In contrast to the simple shear deformations, tensile deformations of a swollen gel can result in variations of the gel volume. Hence, relaxation of the volume fraction of polymer in the course of tensile deformations contributes to the dynamic Young's modulus of the gel and, in general, has to be taken into consideration. The volumetric variations in swollen gels occur due to diffusion of solvent within the gel body and between the gel and the external solution. Therefore, the relative contribution of the volumetric variations to the dynamic Young's modulus depends on the gel size.

To simplify the problem, it is instructive to consider two limiting cases. One case corresponds to the situation when the volumetric relaxation is so fast that it can be taken as instantaneous. This scenario is characteristic of sufficiently small gel samples and slow deformations. In Section S4 of the SI, we calculate the dynamic bulk modulus K_ω in the limit of instantaneous volumetric relaxation, and then use eqs. (16)-(18) to obtain the dynamic Young's modulus, E_ω.

Another characteristic limit corresponds to the situation when variations in the volume of a swollen gel can be neglected as, for example, in the case of sufficiently large gel samples and fast deformations. Absence of variations in volume is effectively equivalent to the gel's incompressibility when the bulk modulus is very high. In the latter case, the dynamic Young's modulus of the gel is determined solely by the dynamic shear modulus (see eq. (16)) and $E_\omega = 3G_\omega$.

D. Model parameters

The model parameters are chosen as in our previous study[11] and are discussed briefly here. The subchains between the cross-links contain $n+l$ Kuhn segments with $n=4$ and $l=8$, and the dangling chains contain $m=2$ Kuhn segments (see Fig. 2). The volume fraction of polymer in the as-fabricated sample is taken to be $\phi_0=0.129$, and the corresponding cross-link density is determined according to the equation $c_0 v_0=\phi_0 a_0 b^{-1}(n+l+m)^{-1}=1.84\times10^{-3}$ with the size of a monomeric unit $a_0=2\text{Å}$ and the Kuhn length $b=10\,\text{Å}$.[5–7,16]

We assume that the probability for the rupture rate in both the loops and the reactive ends of the dangling chains are similar; hence, the rate constant for bond rupture is assumed to be equal to the rate constant for unbinding, $k_r^{(0)}/k_{uB}^{(0)}=1$. Further, the rate constant of folding relative to that of bond rupture at zero force , and the ratio of the rate constant of complex formation and that of the unbinding at zero force was set to $k_f^{(0)}/k_r^{(0)}=200$ and $K_0/k_{uB}^{(0)}=2\times10^4$ respectively. Furthermore, the rate constant of folding relative to that of bond rupture at zero force , and the ratio of the rate constant of complex formation and that of the unbinding at zero force was set to $k_f^{(0)}/k_r^{(0)}=200$ and $K_0/k_{uB}^{(0)}=2\times10^4$, respectively. For more details on how the choice of rate constants affects the behavior of the gel systems, we refer the reader to Sec. S6 in the SI.

The force sensitivity parameters for the rate constants of bond rupture and unbinding were set to $\gamma_R=1.5$ and $\gamma_{uB}=0.75$, respectively. To capture the temperature dependent (LCST) behavior of the gel, we use the known experimental values that characterize poly(N-isopropylacrylamide) (pNIPAAm) gel.[8] Correspondingly, the polymer-solvent interaction is taken to be $\chi(\phi,T)=\chi_0(T)+\chi_1\phi$, where $\chi_0(T)=h(T_0+T)^{-1}-s$ with $h=-902.44$, $s=3.4163$, $T_0=273.15$, and $\chi_1=0.518$.[8]

For the affine deformations, the degree of swelling (λ in Fig. 3a) is equal to the chain extension, so the same notation is used for both values. The degree of gel swelling λ is defined as the lateral extension of the gel sample i.e., $\lambda = L / L_0$ where L is the length of the gel sample along the specified direction and L_0 is the length of the reference gel.

We first consider the calculations of the equilibrium moduli for the four different gel systems shown in Fig. 2. We also perform single-element ($1\times1\times1$ units) gel lattice spring model (gLSM) simulations to further verify our analytical calculations. The details of the gLSM formulation are given in Section S3 of the SI.

III. Results and Discussion

A. Determining the equilibrium moduli: effect of varying temperature

We first determine the equilibrium behavior of the four different gel systems depicted in Fig. 2. Figure 3a shows the equilibrium degree of swelling, λ, as a function of temperature for the LCST gel, which shrinks with increasing temperature. (Note the unfolding and (no)binding case marked in (blue) red is also presented in Biswas *et al.*[11].) Using the gLSM, we determine λ for the equilibrated gels in the temperature range $T = 15°\text{C}$ to $T = 45°\text{C}$. The gels are $1\times1\times1$ units in size, corresponding to samples that are $40\,\mu\text{m}$ on each side.

In System I (black), the loops are permanently in the unfolded state ($p_U = 1$ and $p_B = 0$). The exposure of "hidden" chain length with the unfolding of loops enables this system to show the greatest degree of swelling. Since the ends of the dangling chains are inert in this system, the gel does not exhibit self-reinforcement. Among the four systems, this is the most open or unconstrained system since the polymer chains are bound only at the permanently crosslinked sites. System II (blue) is similar to System I (black), except that the loops can undergo a folding and unfolding transition, but the ends of the dangling chains remain inert. Because only half of the

subchains contain loops, and these loops can fold with a certain probability, p_U, the blue curve shows a slightly lower degree of swelling than that for System I (black). Here, p_U is obtained from solving for the steady state solution of eq. (1) and $p_B = 0$.

In System III, the dangling ends are again inert ($p_B = 0$), but the loops are permanently folded, i.e., the transition from folding to unfolding is forbidden. Thus, the $p_U = 0$. The number of Kuhn segments participating in the elasticity of the network is reduced to *n* segments since the *l* segments in the folded loops are "wasted". Below T_c, the swelling of the LCST gel leads to a buildup in the internal force acting on the loops (even in the absence of applied force). As the temperature is lowered well below T_c (Fig. 3a), the permanently folded loops do not unfold and thus, these loops resist the swelling, as can be seen from the lower values of the swelling curve for System III (in green) as compared to System I (black) and System II (blue).

In System IV, the loops can undergo reversible folding and unfolding, and the dangling linkers with reactive ends can bind to the exposed "cryptic" sites. Here, p_U and p_B are obtained from solving the kinetic equations, eqs. (1) and (2), for the steady state solution. These gels are the most tunable and show the greatest self- reinforcing behavior among the four systems.

There are two noticeable differences between the cases involving binding (red) and no binding (black, blue, green) units. With binding present, there is a shift in the volume phase transition temperature, T_c, to lower values, and a decrease in the lateral extension of the gel (Fig, 3a). Both the latter effects are due to the presence of the temporary cross-links between the exposed cryptic sites (on the opened loops) and the reactive dangling ends. These cross-links act as "struts" that inhibit the swelling of the gel. In effect, the struts increase the stiffness of the network and thus, the gel undergoes a self-stiffening in response to the decrease in temperature.

The effect of these changes in the gel's internal structure on the mechanical properties of the system can be quantified by calculating the equilibrium elastic moduli as functions of the temperature, T. The numerical solution for the shear modulus, eq. 19, is shown in Fig. 3b. The Young's modulus is calculated indirectly by first obtaining the solution for the bulk modulus. The equilibrium bulk modulus is obtained as detailed in Section S4 of the SI. Inserting the calculated values of the shear and bulk moduli into eq. 16 yields the Young's modulus (Fig. 3c). As a means of verifying these results, we also plot the moduli obtained from the single element gLSM simulations (marked with points). Note that the results from the gLSM simulation show quantitative agreement with the numerical values calculated from the linearized theory. Comparison of Figs. 3b and 3c show that the plots for the shear and Young's moduli versus temperature exhibit similar trends for all $T < T_c$.

From the plots in Fig. 3, it is also evident that among the four systems considered here, System I provides the least resistance to deformation. Hence, we use the shear modulus of System I at $T = 15°\mathrm{C}$ as the reference value, denoted G_{ref}, for all the elastic moduli calculated here. We estimate $G_{ref} \sim 33\,\mathrm{KPa}$ at the model parameters used in this study. In Figs. 3b and 3c, the equilibrium values of the shear and Young's moduli for all the systems are rescaled by G_{ref}. Hence, the black line starts at the value of 1 at $T = 15°\mathrm{C}$. The lines thus show the value of the relative moduli as compared to G_{ref}.

Recall that System I is free from folding and binding constraints. The loops in System I are always in the unfolded state and the inert ends of the dangling chains are not reactive and hence, the system does not form the temporary crosslinks that would stiffen the gel. Consequently, among the four systems, System I swells the most and offers the least resistance to deformation; this

behavior is reflected in the lowest value of the equilibrium moduli (black) for both shear and tensile deformation. Unlike System I, the loops in System II can undergo reversible folding and unfolding, but the reactive ends of the dangling chains remain inert. At temperatures below T_c, the swelling of the LCST gel generates internal strain, which causes most of the loops to be in the unfolded state. In this unfolded state, System II behaves similarly to System I. As some fraction of loops in the gel remain in the folded configuration, System II exhibits a greater resistance to deformation than System I, as seen in Figs. 3b and 3c for the equilibrium moduli. Consequently, the shear and bulk moduli of System II (shown in blue) are greater than those in moduli System I (black).

The loops in System III (green) remained permanently folded and thus resist the deformation of the gel; consequently, this sample gives rise to the highest moduli at relatively low temperatures (in green in Figs 3b and 3c). In this range, System IV (red) is softer than System III (green), but stiffer than Systems I (black) and II (blue). There is, however, a temperature, T_s, where the green and red curves cross and switch behavior. This switching can be explained as follows. At temperatures $T < T_s < T_c$, several loops in System IV are unraveled by the swollen gel. The exposed hidden length enables further swelling of the gel, despite the formation of temporary crosslinks between the exposed loops sites and reactive ends.

At temperatures above T_s, however, the less swollen LCST gel is less effective at disrupting the loops and some of the exposed sites remain bound to dangling ends. Both these factors hinder deformation and hence, at these higher temperatures, System IV exhibits a higher modulus than System III (green). The difference in the moduli between the red and green curves is the highest around T_c and decreases as the temperature is shifted away from T_c. Moreover, the largest differences between the equilibrium moduli are evident between the red and black curves

(with no unfolding and no binding). In particular, at T_c : 32°C , the shear modulus of System IV(red) is 21% higher than the modulus of System I (black), and the Young's modulus of System IV(red) is ~58% higher than the modulus for System I (black).

B. Determining the dynamic moduli: effect of varying frequency at given temperatures

To further characterize the system, we calculate the frequency-dependent response of the gels to vibratory deformation and determine the storage modulus of the four systems for both shear and tensile deformation. As noted above, the storage modulus characterizes the energy stored in the material. The expressions used to numerically calculate the frequency-dependent moduli are given in Section S4 of the SI. The numerical solutions characterizing the equilibrium behavior of the systems are used to obtain the values of the storage moduli for both shear and tensile deformation.

1. **Storage shear moduli.** The numerical solution for the storage shear modulus (eq. (17)) is shown in Figs. 4a and 5a. The Young's storage modulus is calculated indirectly by first determining the solutions for the bulk modulus according to eq. (S4.18) in the SI. Inputting these values of the shear and bulk modulus into eq. (16) yields the Young's modulus. Note that the values of the storage shear modulus (G') and storage Young's modulus (E') plotted in Figs. 4 and 5 are normalized to G_{ref} (see above). As an additional validation, the single element gLSM simulation of the simple shear deformation was performed. The results of the gLSM simulation obtained in the case of small deformations are in a good agreement with the linearized theory (see Fig. S2 in the SI).

As seen from the analytical calculations, eq. (17), the storage shear modulus depends only on the unbinding rate constant k_{uB}. Figures 4a and 5a present the storage shear modulus G' of the

four different gel systems as functions of the frequency ω at $T = 22°\text{C}$ and $T = 29°\text{C}$, respectively. We find that the value of the storage modulus is independent of frequency for Systems I, II, and III. The storage modulus is constant and equal to the value of the equilibrium shear modulus of the respective systems. This behavior is due to the fact that in Systems I, II, and III, the reactive ends of the dangling chains are inert and do not undergo binding. Moreover, the storage shear modulus for System I is constant because there is no structural relaxation in this system.

On the other hand, the dynamic storage moduli for System IV (where the reactive ends of the dangling chains are allowed to undergo binding and unbinding transitions) do show a frequency-dependent behavior. At sufficiently low frequencies, $\omega << k_{uB}^{-1}$, the storage shear modulus is constant (Figs. 4a and 5a), and equal to the equilibrium modulus at a given temperature. As frequency is increased, the storage shear modulus monotonically increases until it levels off at a sufficiently high frequency $\omega >> k_{uB}^{-1}$. The increase in the modulus with an increase in frequency is attributed to the formation of temporary crosslinks in System IV. At $T = 22°\text{C}$, the storage shear modulus of System IV (red) crosses over and above the modulus of System III (green), demonstrating that the bound dangling chains provide additional self-stiffening to the system. At higher frequencies, the storage shear modulus of System IV increases by 66% and 119% as compared to the equilibrium modulus value at $T = 22°\text{C}$ and $T = 29°\text{C}$, respectively.

2. **Storage Young's modulus.** In contrast to the dynamic shear modulus, the dynamic Young's modulus depends on the rate constants for both unfolding and unbinding as shown in the SI (see eqs. (S4.8) and (S4.18)). Figures 4b and 5b present the storage Young's moduli E' as functions of ω at $T = 22°\text{C}$ and $T = 29°\text{C}$, respectively. System I (black) is always unfolded and System III (green) is permanently folded, and neither system contains reactive dangling ends.

Hence these systems do not undergo any transition and do not exhibit any frequency dependence. The values of the storage Young's moduli E' for these cases are equal to their respective equilibrium values.

Although the dynamic shear moduli in System II (blue) remains constant under variations in frequency, the storage Young's modulus does show, albeit small, but a finite variation with frequency. At lower values of frequency, the value of the dynamic modulus remains a constant and is equal to the equilibrium modulus. As frequency is increased further, the value of the modulus increases only incrementally and then saturates to a slightly higher value with increasing frequency. This behavior can be attributed to the formation of folded conformations in System II (blue) as the increase in modulus approaches the value of the modulus of System III, which has permanently folded loops.

For System IV (red), the change in the value of the storage modulus as a function of frequency is seen to be quite large, and is attributed to the formation of temporary crosslinks, as described for the higher value of the storage shear modulus. At $T = 22°\text{C}$, the storage modulus of System IV crosses over that of System III. The latter behavior shows that the temporary crosslinks, which are formed by the bound dangling chains, resist the deformation at higher frequencies. For $T = 29°\text{C}$, the increase in the values of moduli is even larger than at $T = 22°\text{C}$.

At $T = 29°\text{C}$, Figs. 5a and 5b also reveal that the values for the storage moduli for System IV lie above those of System III throughout the frequency sweep, indicating that System IV is stiffer for all values of frequency. While at $T = 22°\text{C}$, for low values of frequency, System III exhibits greater stiffness than System IV. There is a dynamic change in mechanical stiffness between System III and IV based on temperature and frequency. At values of high frequency, the

storage Young's modulus of System IV increases by 60% and 109% compared to their respective equilibrium values at $T = 22°\text{C}$ and $T = 29°\text{C}$.

The storage Young's moduli presented in Figs. 4b and 5b were calculated assuming instantaneous volumetric relaxation. To reveal how relaxation of volume affects the dynamic tensile properties of the swollen gels, we focus on System IV, where both unfolding of the loops and binding of the dangling chains takes place. In Fig. 6, we plot the storage Young's moduli for System IV calculated at $T = 22°\text{C}$ and $29°\text{C}$ in the limiting cases of instantaneous volumetric relaxation and absence of the latter relaxation. The area between the curves representing the two limiting cases at a given temperature is shaded in Fig. 6. The latter figure shows that the storage moduli E' calculated under the assumption of no volumetric relaxation are, first, systematically greater than those obtained in the limiting case of instantaneous relaxation of volume of a swollen gel, and, second, exhibit qualitatively similar behavior as functions of the frequency ω. Recall that the very fast and very slow relaxations of volume of a swollen gel are characteristic for gel samples of sufficiently small and large sizes, respectively (see Section IIC). Thus, at a given temperature, the storage Young's modulus obtained for a realistically sized sample of a swollen gel would lie somewhere in between the two limiting cases, i.e., within a corresponding shaded area shown in Fig. 6.

IV. Conclusions

Through the studies presented here, we could "zoom in" and correlate specific architectural changes in polymer networks to variations in mechanical behavior, and thus obtain useful structure-property relationships for these multi-component gels. The gels contained salient features that are common to a majority of networks: unfolding loops that expose "hidden length"

and release new binding sites; dangling chains with reactive or inert end groups; and "wasted" closed loops. All these features affect the material's mechanical response to deformation. To quantify this response, we derived expressions for the equilibrium and dynamic values of the elastic moduli that explicitly take into account the different architectural features. These models allowed us to pinpoint how different binding and folding events contribute to the material's response to shear and tensile deformation.

Using the analytical calculations and numerical simulations, we determined the elastic moduli for the four systems in Fig. 2. In Systems I-III, the binding transition does not take place, whereas in System IV, both the binding and folding transitions occur. For the chosen model parameters, we observed that System I with its permanently unraveled loops was the softest among all the systems (followed by System II). In particular, System I had the lowest equilibrium moduli for both shear and tensile deformations, and did not show any frequency dependence on the moduli.

For both the equilibrium shear and Young's moduli, there exists a crossover temperature T_S beyond which the modulus values are exchanged. Note that T_S is different for the shear modulus and the Young's modulus. For $T < T_S$, the gel system with permanently folded loops (System III) exhibited a higher modulus than System IV. In this temperature range, the closed loops were responsible for resisting the swelling of the gel. Above T_S, however, the transient crosslinks became more effective than the closed loops in resisting the deformation of the gel. This transient crosslinks acted as struts that reinforced the mechanical stiffness of the gels.

We also investigated the frequency-dependent response of the systems in the limit of small deformation. The isothermal frequency scans for the shear storage moduli showed no dependence om frequency for Systems I-III. For the storage Young's modulus, the sample undergoing folding

and binding (System IV) showed a significant dependence on frequency as the moduli depends on the kinetic rate constants of folding and binding.

In contrast to the other systems, System IV encompasses the greatest degree of tunability as demonstrated by the wide range of moduli the system exhibited when compared with Systems I to III. Hence, System IV provides a useful structural framework for altering the macroscopic mechanical properties of a network through localized, molecular scale manipulations. Given that loops and dangling ends are ubiquitous in polymer networks, the studies reveal how these defects can be used to greatest advantage. The findings also reveal the key role that dynamic bonds play in dictating the global mechanical behavior.

Conflicts of Interest

There are no conflicts of interest to declare.

Acknowledgements

ACB gratefully acknowledges financial support from DOE grant number DE-FG02-02ER45998 for the development of the theoretical model and ARO grant number W911NF1910388 for the development of the computer simulations.

References

1 F. Ikkai and M. Shibayama, *J. Polym. Sci. Part B Polym. Phys.*, 2005, **43**, 617–628.

2 H. Zhou, J. Woo, A. M. Cok, M. Wang, B. D. Olsen and J. A. Johnson, *Proc. Natl. Acad. Sci. U. S. A.*, 2012, **109**, 19119–24.

3 E. Klotzsch, M. L. Smith, K. E. Kubow, S. Muntwyler, W. C. Little, F. Beyeler, D. Gourdon, B. J. Nelson and V. Vogel, *Proc. Natl. Acad. Sci. U. S. A.*, 2009, **106**, 18267–72.

4 O. Peleg, T. Savin, G. V. Kolmakov, I. G. Salib, A. C. Balazs, M. Kröger and V. Vogel, *Biophys. J.*, 2012, **103**, 1909–1918.

5 V. V. Yashin and A. C. Balazs, *Science*, 2006, **314**, 798–801.

6 V. V. Yashin and A. C. Balazs, *J. Chem. Phys.*, 2007, **126**, 124707.

7 O. Kuksenok, V. V. Yashin and A. C. Balazs, *Phys. Rev. E - Stat. Nonlinear, Soft Matter Phys.*, 2008, **78**, 041406.

8 S. Hirotsu, *J. Chem. Phys.*, 1991, **94**, 3949.

9 Y. Ma, M. Hua, S. Wu, Y. Du, X. Pei, X. Zhu, F. Zhou and X. He, *Sci. Adv.*, 2020, **6**, eabd2520.

10 L. D. Landau and E. M. Lifshitz, *Theory of elasticity*, Butterworth-Heinemann, 1986.

11 S. Biswas, V. V. Yashin and A. C. Balazs, *Soft Matter*, 2020, **16**, 5120–5131.

12 I. G. Salib, G. V. Kolmakov, B. J. Bucior, O. Peleg, M. Kröger, T. Savin, V. Vogel, K. Matyjaszewski and A. C. Balazs, *Langmuir*, 2011, **27**, 13796–13805.

13 B. V. S. Iyer, V. V. Yashin and A. C. Balazs, *New J. Phys.*, 2014, **16**, 075009.

14 S. Biswas, V. V. Yashin and A. C. Balazs, *Soft Matter*, 2018, **14**, 3361–3371.

15 A. D. Drozdov, *Finite Elasticity and Viscoelasticity*, World Scientific, Singapore, 1996.

16 D. Magerl, M. Philipp, E. Metwalli, P. Gutfreund, X.-P. Qiu, F. M. Winnik and P. Müller-Buschbaum, *ACS Macro Lett.*, 2015, **4**, 1362–1365.

Figure captions

Figure 1 Schematic of a polymer network (in green) containing loops and dangling chains. The cross-links are shown in grey solid circles. The loops in permanently folded state or permanently unfolded state (chemically inert) are shown in black solid circles. The loops with reactive labile bonds are shown in blue when bonded. The reactive ends of the dangling chains (yellow) can

undergo binding with the exposed ends of the loop (red) while the ends of the dangling chain that are treated as chemically inert are shown with black solid circles.

Figure 2 Schematic of the four different gel systems. In System I, the structural elements i.e. the loops are permanently in the unfolded state and the dangling chains are chemically non-reactive, so they cannot participate in binding. System II depicts the gel network where the ends of the dangling chains are chemically inert but the cryptic sites in the loops are reactive, so the loops can undergo the reversible folding-unfolding transformations. In System III, the loops are permanently in a folded state and cannot undergo folding-unfolding transition. The dangling chain thus cannot find exposed cryptic sites and the system also does not undergo binding-unbinding transition. In System IV, both the structural elements (loops and dangling chains) have chemical reactive ends. The cryptic sites can undergo folding-unfolding transition and the ends of the dangling chains and can bind reversibly to the exposed cryptic sites.

Figure 3 (a) The lateral extension (b) shear modulus (G_0) and (c) Young's modulus (E_0) of the gel at equilibrium as a function of temperature for the gel systems I - IV. Note that the difference in the degree of swelling between the bound (system IV) and the other systems I-III is greater near the transition temperature. The model parameter values are given in the text. The lines show the numerical solution of eq. (7) equated to zero i.e. at the steady state obtained using *Mathematica*™. The symbols show the numerical solution obtained using the gLSM code applied for a single gel element in the long time limit. The moduli in (b) and (c) are scaled with respect to the shear modulus value of the gel system I, G_{ref}, at 15°C . Hence, the shear moduli plot of gel system I starts from the value of 1 at 15°C .

Figure 4 (a) The storage shear modulus (G') and (b) storage Young's modulus (E') of the four different gel systems as functions of the frequency (ω) at $T = 22°\text{C}$. The moduli values are scaled with G_{ref} . The values of the parameters are given in the text. The lines show the numerical solution obtained using *Mathematica*™ for the given set of frequencies in the range of $[10^{-2},10^{3}]$. The storage modulus is independent of frequency and equal to the value of the equilibrium shear modulus for Systems I, II, and III. For system IV, the storage shear moduli depends on the binding rate constant and varies with frequency. As frequency is increased, the storage shear modulus monotonically increases until it becomes a constant at a sufficiently high frequency. Similarly, in (b) the storage Young's moduli (E') of the gel for system I and III remains constant. The storage Young's modulus depends on both unfolding as well as unbinding rate constant. The moduli of System II shows a very small variation with frequency. The Young's modulus for system IV remains constant for low frequency and equal to the equilibrium value of the moduli but monotonically increases until it saturates at a sufficiently high frequency.

Figure 5 (a) The storage shear modulus (G') and (b) storage Young's modulus (E') of the four different gel systems as functions of the frequency (ω) at $T = 29°\text{C}$. The moduli values are scaled with G_{ref} . The model parameter values are given in the text. The lines show the numerical solution obtained using *Mathematica*™ for the given set of frequencies in the range of $[10^{-2},10^{3}]$. The storage modulus is independent of frequency and equal to the value of the equilibrium shear modulus for Systems I, II, and III. For system IV, the storage shear moduli depends on the binding rate constant and varies with frequency. As frequency is increased, the storage shear modulus monotonically increases until it becomes a constant at a sufficiently high frequency. Similarly, in

(b) the storage Young's moduli (E') of the gel for system I and III remains constant. The storage Young's modulus depends on both unfolding as well as unbinding rate constant. The moduli of System II shows a very small variation with frequency. The Young's modulus for system IV remains constant for low frequency and equal to the equilibrium value of the moduli but similar to the storage shear modulus monotonically increases until it saturates at a sufficiently high frequency. At $T = 29°\mathrm{C}$, the moduli values of system IV are higher than the moduli values of system III for all frequencies.

Figure 6 The storage Young's moduli (E') versus frequency (ω) for System IV at $T = 22°\mathrm{C}$ (red) and $29°\mathrm{C}$ (orange) in the limiting cases of instantaneous volumetric relaxation denoted by solid line and absence of volumetric relaxation (dashed line). The shaded area between the curves represent that a realistically sized sample of a swollen gel would lie between these two limiting cases at a given temperature.

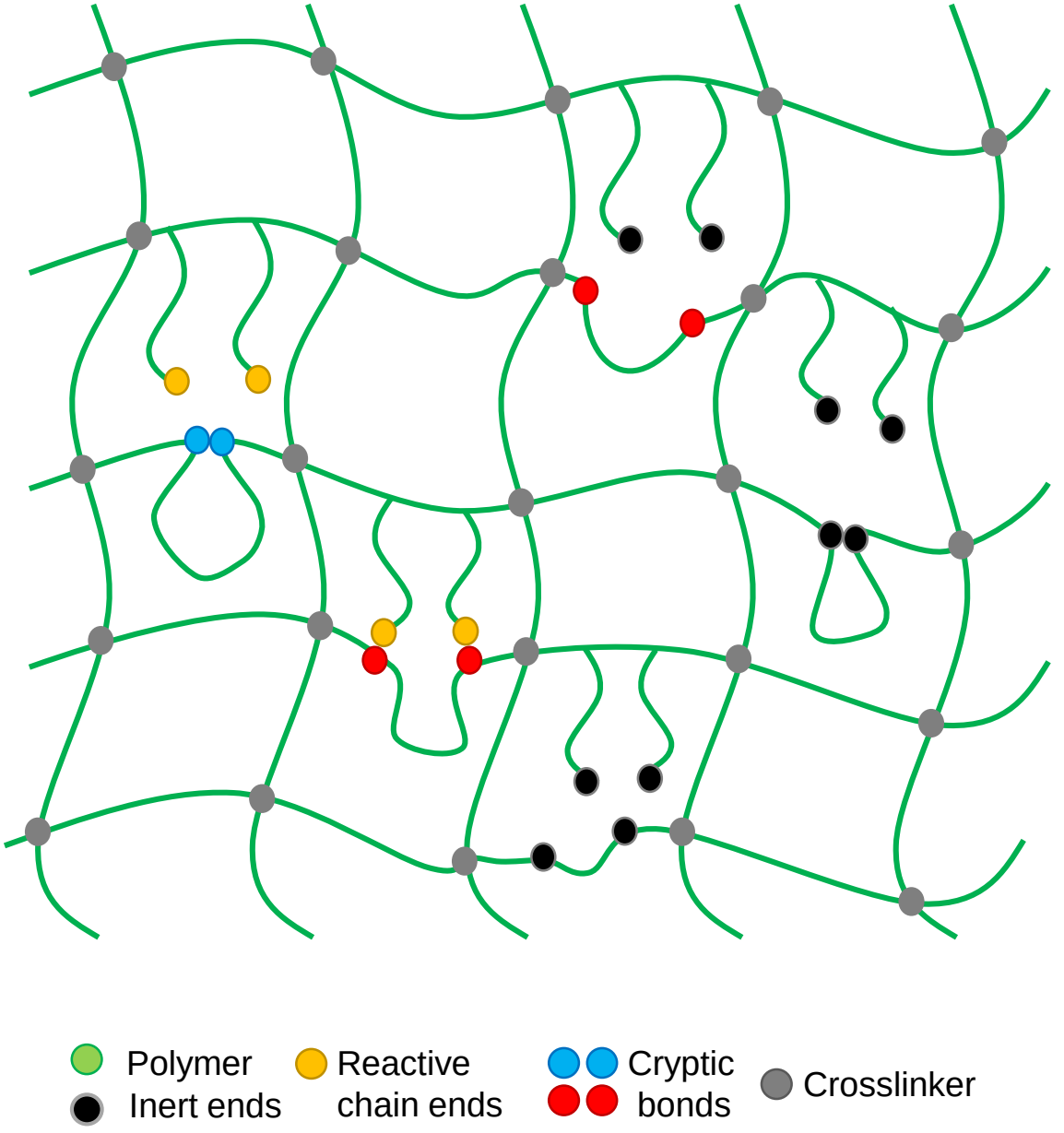
Polymer
Inert ends
Reactive
chain ends
Cryptic
bonds
Crosslinker

Figure 1

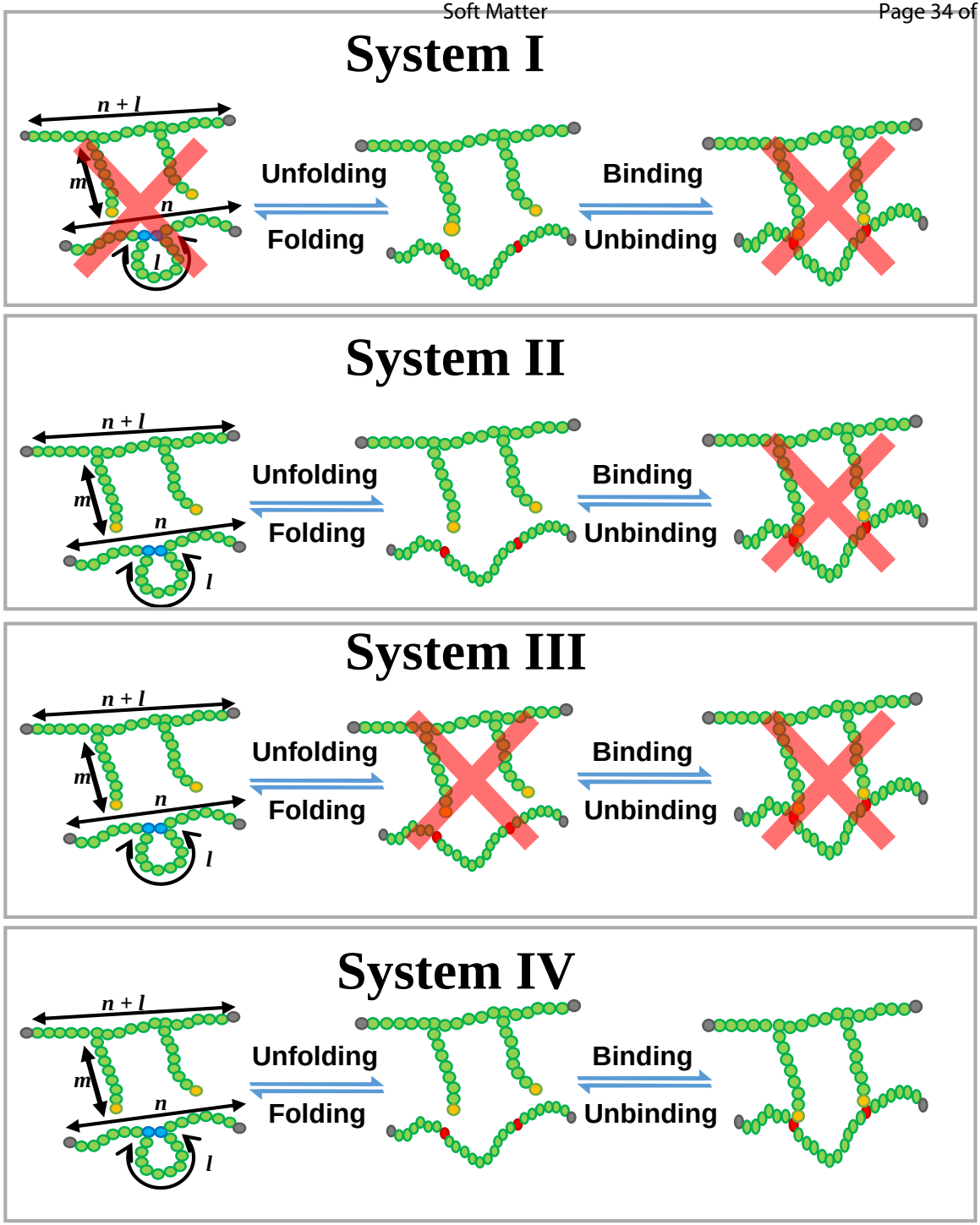
System I
n + l
m
n
l
Unfolding
Folding
Binding
Unbinding
System II
n + l
m
n
l
Unfolding
Folding
Binding
Unbinding
System III
n + l
m
n
l
Unfolding
Folding
Binding
Unbinding
System IV
n + l
m
n
l
Unfolding
Folding
Binding
Unbinding
Polymer
Reactive chain ends
Cryptic bonds
Crosslinker

Figure 2

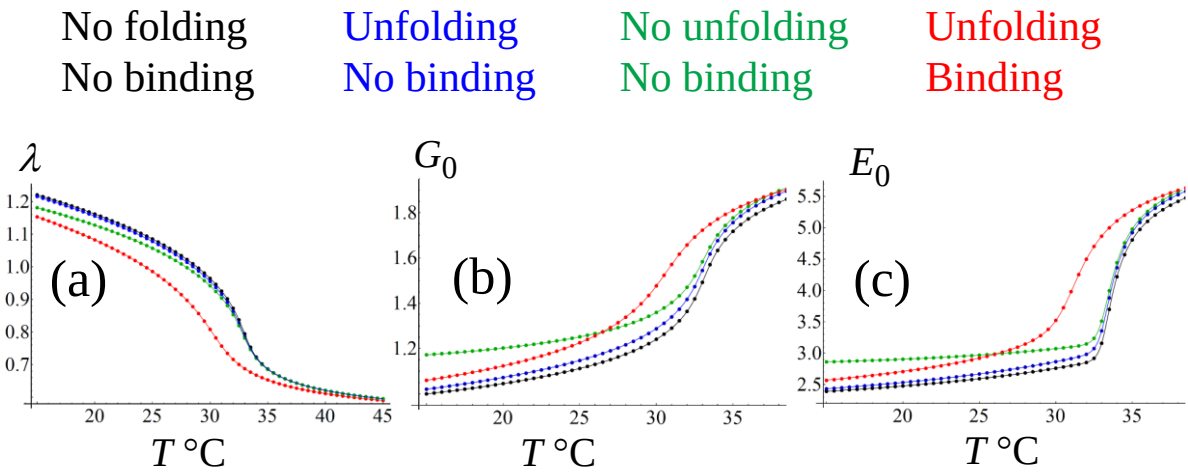
No folding
No binding
Unfolding
No binding
No unfolding
No binding
Unfolding
Binding
λ
(a)
T °C
G0
(b)
T °C
E0
(c)
T °C

Figure 3

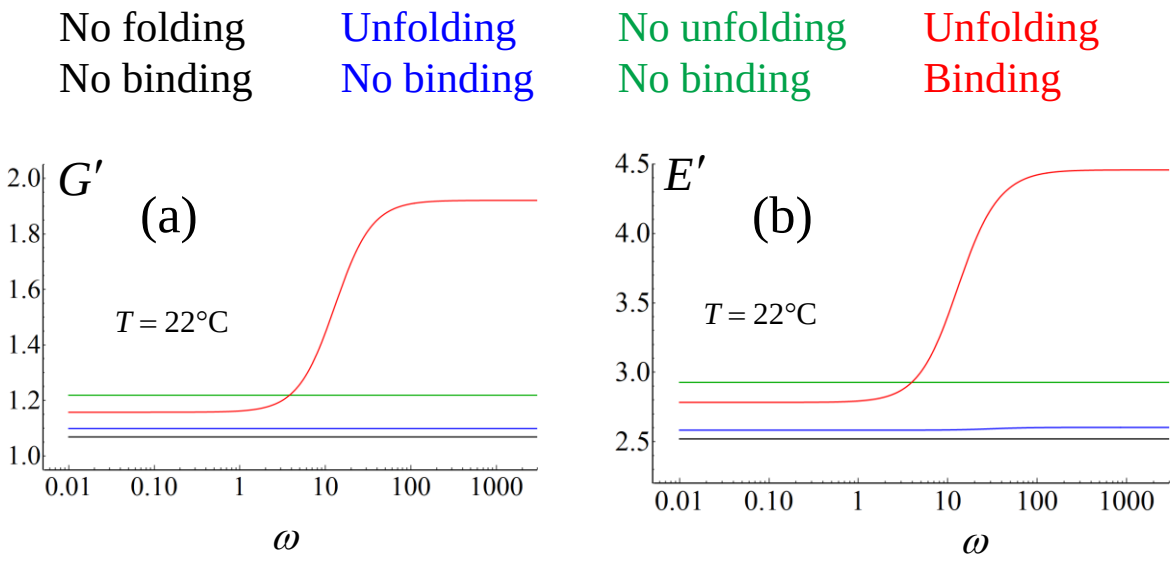
No folding
No binding
Unfolding
No binding
No unfolding
No binding
Unfolding
Binding
G′
(a)
T = 22°C
2.0
1.8
1.6
1.4
1.2
1.0
0.01
0.10
1
10
100
1000
ω
E′
(b)
T = 22°C
4.5
4.0
3.5
3.0
2.5
0.01
0.10
1
10
100
1000
ω

Figure 4

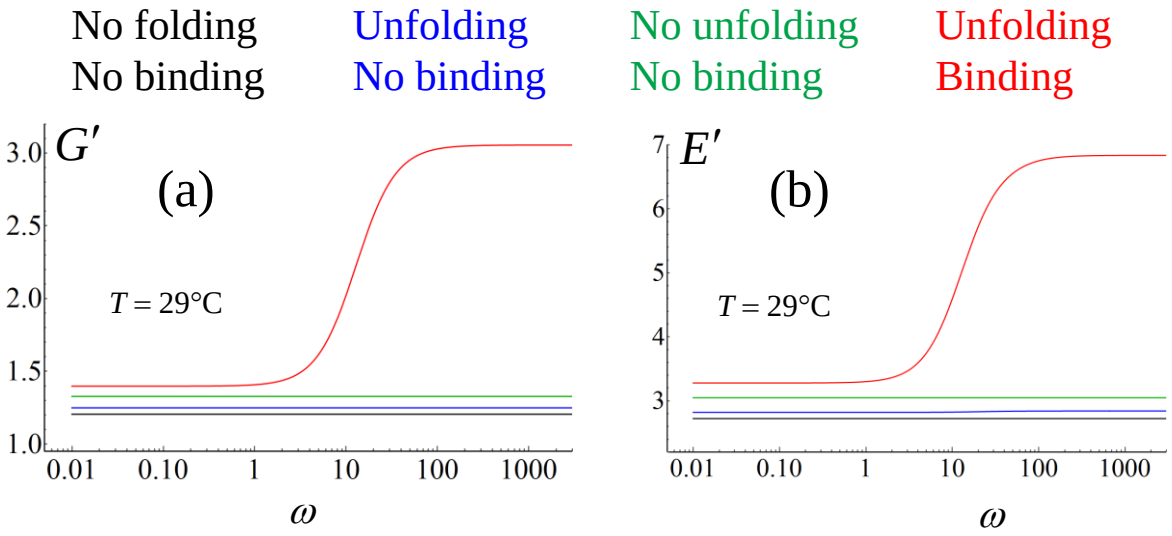
No folding
No binding
Unfolding
No binding
No unfolding
No binding
Unfolding
Binding
G′
(a)
T = 29°C
3.0
2.5
2.0
1.5
1.0
0.01
0.10
1
10
100
1000
ω
E′
(b)
T = 29°C
7
6
5
4
3
0.01
0.10
1
10
100
1000
ω

Figure 5

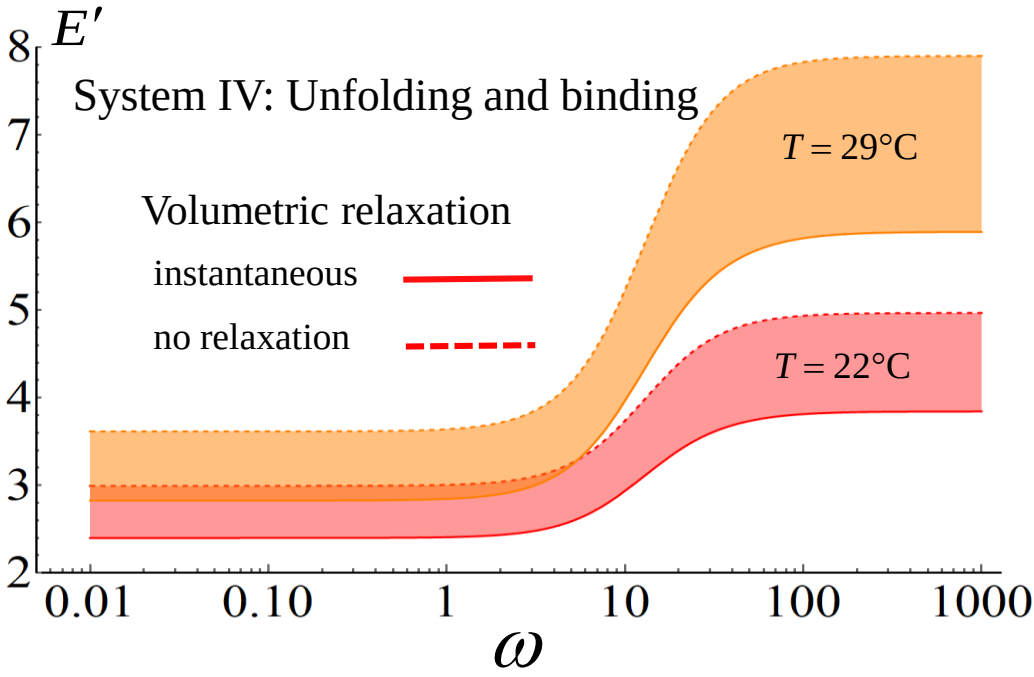
E′
System IV: Unfolding and binding
Volumetric relaxation
instantaneous
no relaxation
T = 29°C
T = 22°C
8
7
6
5
4
3
2
0.01
0.10
1
10
100
1000
ω

Figure 6